

# An Aqueous Rechargeable Formate-Based Hydrogen Battery Driven by Heterogeneous Pd Catalysis\*\*

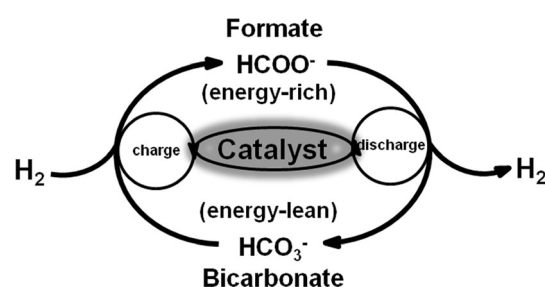
Qing-Yuan Bi, Jian-Dong Lin, Yong-Mei Liu, Xian-Long Du, Jian-Qiang Wang, He-Yong He, and Yong Cao\*

**Abstract:** The formate-based rechargeable hydrogen battery (RHB) promises high reversible capacity to meet the need for safe, reliable, and sustainable  $H_2$  storage used in fuel cell applications. Described herein is an additive-free RHB which is based on repetitive cycles operated between aqueous formate dehydrogenation (discharging) and bicarbonate hydrogenation (charging). Key to this truly efficient and durable  $H_2$  handling system is the use of highly strained Pd nanoparticles anchored on graphite oxide nanosheets as a robust and efficient solid catalyst, which can facilitate both the discharging and charging processes in a reversible and highly facile manner. Up to six repeated discharging/charging cycles can be performed without noticeable degradation in the storage capacity.

Identifying and building a sustainable energy system are two of the most significant issues facing modern society.<sup>[1]</sup> Current energy systems that are mostly based on fossil fuels, which have limited supply and considerable negative environmental impact, should ideally be replaced with systems based on renewable fuels. To make alternative energy solutions more competitive than existing ones, the challenge of reversible energy storage and delivery must be solved to address fluctuations in demand and supply.<sup>[1,2]</sup> Hydrogen is a very flexible energy carrier and considered to be a globally accepted clean energy feedstock.<sup>[3]</sup> However, lack of safe, efficient, and economical  $H_2$  storage technologies hinders the viability of a hydrogen-based economy.<sup>[4]</sup> Storing  $H_2$  in chemical bonds is attractive because of the high energy density by weight of chemical fuels. In this context, one of the most promising strategies to store hydrogen entails the interconversion of  $H_2$  and  $CO_2$ .<sup>[5]</sup> This approach offers

direct access to regenerative energy carriers based on waste material from the energetic use of fossil fuels, opens a possible route to convert abundantly available, inexpensive, and renewable  $CO_2$  into a variety of liquid fuels,<sup>[5a-c,e]</sup> and is discussed as a potential option for the development of efficient sustainable energy supply chains.<sup>[5c]</sup> A full optimization of the relevant reaction pathway is believed to be an essential step toward the realization of a carbon-neutral energy future. The vital challenge for implementing such advanced energy storage concepts lies in the development of new, innovative, economically feasible, and reliable catalytic methods that do not only store  $H_2$  at high energy density but that can operate reversibly under realistic working conditions.<sup>[6]</sup>

As a result of an ever-increasing demand for mobile devices and the continued search for new improved energy storage technologies for both transportation and grid-scale needs, a compact and regenerative  $H_2$  storage system that can allow hydrogen uptake and release under identical conditions is a highly desired goal.<sup>[7]</sup> Such a battery-like  $H_2$  handling system, namely rechargeable hydrogen battery (RHB),<sup>[8]</sup> would be especially attractive in terms of its potential to decouple energy production and energy consumption with respect to both space and time, a key issue in relation to the integration of renewable energies into our future energy scenarios. One promising storage medium identified in this regard is the formate/bicarbonate redox couple (Scheme 1),



**Scheme 1.** Aqueous RHB based on the formate/bicarbonate system.

which has several desirable properties that makes it an attractive candidate for an enabling RHB system.<sup>[9]</sup> First, a thermodynamically reversible and essentially water-based  $H_2$  storage system can be achieved at near ambient conditions through the chemical equilibrium of  $HCOO^- + H_2O \leftrightarrow H_2 + HCO_3^-$ . Second, it can be directly adapted to downstream applications such as fuel-cell-based technologies for clean

[\*] Dr. Q. Y. Bi, J. D. Lin, Dr. Y. M. Liu, Prof. Dr. H. Y. He, Prof. Dr. Y. Cao  
Department of Chemistry, Shanghai Key Laboratory of Molecular Catalysis and Innovative Materials, Collaborative Innovation Center of Chemistry for Energy Materials, Fudan University  
Shanghai 200433 (P. R. China)  
E-mail: yongcao@fudan.edu.cn

Dr. X. L. Du, Prof. Dr. J. Q. Wang  
Shanghai Institute of Applied Physics, Chinese Academy of Sciences  
Shanghai 201800 (P. R. China)

[\*\*] This work was supported by the National Natural Science Foundation of China (21273044, 21473035), the State Key Basic Research Program of PRC (2009CB623506), the Research Fund for the Doctoral Program of Higher Education (2012007000011), the China Postdoctoral Science Foundation (2014M551314), and the Science & Technology Commission of Shanghai Municipality (08DZ2270500).

Supporting information for this article is available on the WWW under <http://dx.doi.org/10.1002/anie.201409500>.

power generation, given the ultraclean nature of the resulting H<sub>2</sub> stream (essentially free of CO<sub>x</sub> and volatile organic compounds).<sup>[10]</sup> To realize the full potential of this particular energy storage system, the overall process should be performed in the same vessel using one single catalyst. Two very recent reports describe the feasibility of using a homogeneous Ru catalyst to enable a reversible HCOONa/NaHCO<sub>3</sub>-based H<sub>2</sub> storage.<sup>[9]</sup> However, apart from the practical inconvenience arising from the use of sophisticated ligands, the application of these systems is greatly constrained by limited durability and deliverable capacity.

Herein, we demonstrate the possibility to set up a viable and truly rechargeable hydrogen storage device, simply by applying a novel heterogeneous Pd-based catalyst capable of facilitating efficient and reversible interconversion of formate and bicarbonate in aqueous solution under mild and practical conditions. The key to the unprecedented hydrogen storage/release efficiency is an integrated development and optimization of the catalytic metal and the underlying support that exploit the principles of metal–support synergy involving carbon-based “flat-mat” materials such as reduced graphite oxide (r-GO) nanosheets as the support as well as the microstructural properties of firmly anchored Pd nanoparticles (NPs) for reactivity control. The results not only show a benchmark example of the metal–graphite-based hybrid material used as an incredibly efficient, robust, and durable catalyst in practical hydrogen release and storage but also the benchmark example of the H<sub>2</sub> handling system for a future sustainable energy supply.

We began our research by exploring the decomposition of potassium formate (HCOOK, PF) in neat water. The decomposition of aqueous PF may proceed through simple dehydrogenation, producing H<sub>2</sub> and KHCO<sub>3</sub>. At high PF conversions, observation of CO<sub>2</sub> as a secondary decomposition product derived from a partial transformation of bicarbonate to carbonate is also expected. The series of catalysts that were examined in the preliminary study of their catalytic activity toward PF dehydrogenation is summarized in Table 1. The preparation procedure for these noble metal

catalysts and relevant characterization data are provided in the Supporting Information (SI). Importantly, in line with our previous research on low temperature formate activation,<sup>[11]</sup> preliminary tests have shown that some of the catalysts used, such as Au/CeO<sub>2</sub>, Au/ZrO<sub>2</sub>, and Pd/C, exhibit prominent catalytic activity for transfer reduction of aldehydes with aqueous PF (Table S1). We therefore set out to test these Au- and Pd-based catalysts for PF dehydrogenation. For these initial assays the conditions studied were 80 °C, 4.8 M aqueous PF, and a catalyst loading of 0.0265 mol % (the amount of the active metal species relative to the substrate). The extremely low catalyst loading employed in these screening assays is noteworthy. Surprisingly, the Au catalysts tested were not active at all (Table 1, entries 1 and 2). Of the various catalysts examined, only Pd deposited on carbon-based materials showed notable activity with appreciable turnover frequency (TOF, over the first 20 min). In particular, the use of reduced graphite oxide as a support (Pd/r-GO) afforded the highest activity, providing an impressive initial TOF of 5420 h<sup>-1</sup> for exclusive H<sub>2</sub> evolution (Table 1, entry 3). Already, this result represents the best H<sub>2</sub> production efficiency ever reported for dehydrogenation of aqueous formates (Table S2).<sup>[9,12]</sup>

Pd/r-GO is a material in which palladium from PdCl<sub>2</sub> has been deposited onto solution-processable GO by a one-step co-reducing method (Scheme S1).<sup>[13]</sup> Owing to their superior electron mobility, considerable surface area, and chemical tunability, GO and related carbon nanostructures have emerged as a new class of very promising functional materials, especially in sensing, optoelectronics, fuel cells, and related electrochemical energy conversion applications.<sup>[14]</sup> By serving as a unique carbon-based matrix, the GO sheets could be applied for heterogeneous catalysis by anchoring metal NPs on its surface.<sup>[14c,15]</sup> However, approaches for growing narrowly distributed NPs effectively in the presence of GO sheets without the use of capping agents are still rare. Upon using NaBH<sub>4</sub> as the reducing agent, we have been able to directly introduce stabilizer-free Pd NPs on the surface of reduced GO nanosheets at room temperature. A typical TEM image (Figure S1) shows spherical and uniform Pd particles that are ca. 2.4 ± 0.1 nm in size dispersed on the r-GO sheets with only a small degree of particle aggregation. The XPS analysis confirmed the predominant presence of Pd<sup>0</sup> on r-GO (Figure S3). In contrast to the samples in which Pd with an identical metal loading (5 wt % Pd based on ICP analysis) is supported on conventional carbon-based materials or metal oxides, the Pd/r-GO hybrid exhibits remarkable activity toward formate decomposition to yield H<sub>2</sub> (Table 1, entries 4–8). Importantly, controls using pristine r-GO nanosheets as support for Au, Ir, Pt, Ru, and Rh metals exhibit no PF dehydrogenation activity (Table S3), that is, the catalytic properties of Pd/r-GO are derived from the combination of Pd NPs and r-GO.

It is well known that the enhanced catalytic activity of metal particles induced by support materials can in general be attributed to either geometric or electronic effects.<sup>[16]</sup> Given the quite similar average particle size and chemical composition of Pd surfaces seen in the three carbon-supported samples (see the TEM and XPS data provided in the SI), one possibility is a lattice mismatch between the Pd “domain” and

**Table 1:** Study of various solid catalysts for the H<sub>2</sub> generation from aqueous HCOOK.<sup>[a]</sup>

Entry	Catalyst	Metal loading [wt %] <sup>[b]</sup>	Particle size [nm] <sup>[c]</sup>	V <sub>H<sub>2</sub></sub> [mL] <sup>[d]</sup>	TOF [h <sup>-1</sup> ] <sup>[e]</sup>
1	Au/CeO <sub>2</sub>	1	1.9	0	–
2	Au/ZrO <sub>2</sub>	0.8	1.8	0	–
3	Pd/r-GO	5	2.4	408	5420
4	Pd/C	5	2.6	92	1241
5	Pd/XC-72	5	2.4	26	379
6	Pd/CNTs	5	2.3	32	438
7	Pd/TiO <sub>2</sub>	5	2.6	12	204
8	Pd/Al <sub>2</sub> O <sub>3</sub>	5	3.2	16	285
9 <sup>[f]</sup>	Pd/r-GO	1	1.8	426	11 299
10 <sup>[f]</sup>	Pd/r-GO	2	1.9	345	8972

[a] Reaction conditions: 5 mL scale of 4.8 M aqueous HCOOK, 6.4 μmol metal, 80 °C. [b] Determined by inductively coupled plasma (ICP) bulk composition analysis. [c] Evaluated by TEM. [d] Volume of H<sub>2</sub> gas generated in 1 h. [e] Initial TOF measured within the first 20 min. [f] 3.2 μmol Pd. CNTs = carbon nanotubes.

the underlying support surface that may cause an isomorphic (structural) effect on the electronic structure of Pd. The created expansion or contraction in lattice parameters of Pd at the interface, also frequently known as “lattice microstrain”,<sup>[17]</sup> could result in higher activity. We thus checked the lattice strains of these carbon-supported Pd catalysts by synchrotron-radiation-based XRD (Figure S12).<sup>[18]</sup> Indeed, it was found that the dehydrogenation activity of these catalysts critically depends on the degree of lattice expansion in the corresponding Pd crystals, stressing the significance of the r-GO support in providing a suitable catalytic interface between the Pd NPs and the reaction media. This scenario was further corroborated by the examination of a separate set of Pd/r-GO samples with systematically varied Pd content, wherein a strong positive linear correlation of the lattice microstrain in the Pd NPs with their catalytic dehydrogenation activity was identified (Figure S12). Taken together, these results highlight the critical importance of tuning the lattice distortion of supported Pd NPs to facilitate crucial formate activation under mild aqueous conditions. More specifically, the fact that the r-GO support can substantially facilitate the creation of highly strained Pd NPs appears to be the key factor for achieving high activity in the PF dehydrogenation.

Consistent with the inference noted above, it is possible to further improve the dehydrogenation efficiency by progressively decreasing the Pd loading in the Pd/r-GO system. As a result, the 1 wt % Pd/r-GO material possessing the highest level of lattice expansion can deliver an unprecedented TOF up to  $11\,299\text{ h}^{-1}$  (Table 1, entry 9).<sup>[9,12]</sup> Within 2 h, 550 mL of gas can be generated over the 1 wt % Pd/r-GO hybrid (Figure 1), corresponding to almost full conversion (96.6%) of PF into  $\text{H}_2$  and  $\text{KHCO}_3$ . As an illustration that this catalyst remains active for an extended period of reaction time, a continuous stream of 2.2 L of  $\text{H}_2$  can be released from 20 mL of a 4.8 M PF solution within 8 h (Figure S14). In this case, the total turnover number (TON) approached the highest ever-reported value of  $142\,700$ ,<sup>[9,12]</sup> thus further demonstrating the effectiveness of 1 wt % Pd/r-GO for

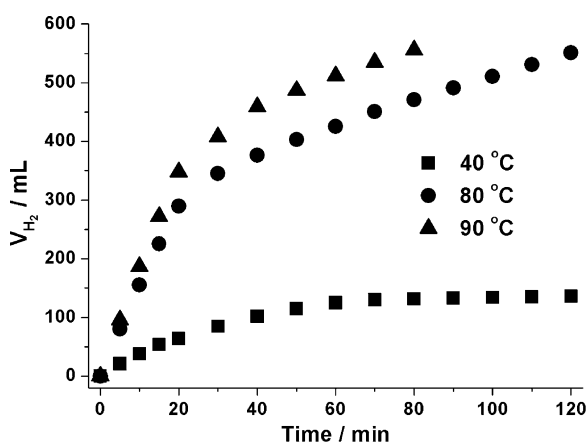


**Figure 1.** Kinetic traces for  $\text{H}_2$  evolution by dehydrogenation of aqueous HCOOK catalyzed by 1 wt % Pd/r-GO. Reaction conditions: 5 mL scale of 4.8 M aqueous HCOOK,  $3.2\ \mu\text{mol}$  Pd.

achieving catalytic PF dehydrogenation, with catalyst loadings that are orders of magnitude lower than those that have previously been employed for this transformation.<sup>[12]</sup> To confirm the identity of the evolved gas, it was introduced into a separate reaction vessel containing styrene, 1 mol % commercial Pd/C (5 wt %), and 10 mL of heptane (see SI). Product analysis of this diagnostic reaction performed at  $40\text{ }^\circ\text{C}$  indicated a clean formation of ethylbenzene (90 % conversion by GC), thereby in turn clarifying that  $\text{H}_2$  was produced from the dehydrogenation reaction. In addition, the headspace gas analysis by GC/MS unambiguously confirmed the exclusive formation of  $\text{H}_2$  without  $\text{CO}_2$  emission in the dehydrogenation reaction.<sup>[19]</sup> A further indication that both PF and water are involved in the dehydrogenation (Scheme S2) came from the observation of an intense signal at  $m/z=3$  (HD) and a diminished signal at  $m/z=2$  upon replacing  $\text{H}_2\text{O}$  with  $\text{D}_2\text{O}$  under otherwise identical reaction conditions (Table S7).<sup>[12a]</sup>

Additional investigation of the various reaction parameters showed that the formate concentration has a profound influence on the reaction outcome (Figure S17). The rates of  $\text{H}_2$  release increased as the PF concentration increased from 1.0 M to 4.8 M; however, higher concentrations ( $> 5.0\text{ M}$ ) were found to have a negative effect on dehydrogenation kinetics, affording a volcano-shaped curve with the highest value at 4.8 M. Despite the reduced activities at higher concentrations of  $> 5.0\text{ M}$ , the catalyst still exhibited enhanced activity compared to previous results even at a high concentration of  $14.2\text{ M}$ ,<sup>[9,12]</sup> which likely provides advantages for practical applications. The most noteworthy aspect, however, is that the reaction did not proceed at temperatures lower than  $30\text{ }^\circ\text{C}$ , thus underscoring the possibility to control  $\text{H}_2$  evolution by varying the reaction temperature in a relatively narrow range. This is indeed the case. Thus, as illustrated in Figure 1, the catalyst showed a very low activity when the reaction was carried out at  $40\text{ }^\circ\text{C}$  ( $\text{TOF} < 2500\text{ h}^{-1}$ ). After a rapid increase of the reaction temperature to  $80\text{ }^\circ\text{C}$ , strong effervescence was immediately observed and the reaction proceeded steadily over time until the PF in the reaction medium was totally consumed. The temperature was then lowered to  $40\text{ }^\circ\text{C}$  ( $25\text{ }^\circ\text{C}$  in the last cycle). This cycle was repeated four times (Figure S18). In all cycles, a reproducible catalytic performance was achieved. This distinct feature, together with the fact that the catalytic system is stable under a wide range of reaction conditions, offers practical advantages over existing methods to establish a more viable hydrogen storage device of great potential for future applications.

Subsequent studies focusing on the comparison with other alkali formates (Table S8) showed that, in contrast to previously reported experiments using Ru-based complexes,<sup>[9]</sup> PF is the substrate of choice for efficient and exclusive  $\text{H}_2$  production under the presented mild aqueous conditions. Interestingly, when the dehydrogenation of PF was performed in the presence of external  $\text{H}_2$  (20–30 bar), a greatly reduced or complete loss of catalytic activity was observed (Figure S21). These results prompted us to examine whether the reverse reaction, i.e., hydrogenation of  $\text{KHCO}_3$  to PF, could be accomplished using the same catalyst (1 wt % Pd/r-GO). It should be emphasized that in the only two related precedents to this work the conversion of bicarbonate to formate







**Keywords:** batteries · energy conversion · hydrogen · lattice strain · Pd catalysis

- [1] a) D. R. Palo, R. A. Dagle, J. D. Holladay, *Chem. Rev.* **2007**, *107*, 3992; b) U. Eberle, M. Felderhoff, F. Schüth, *Angew. Chem. Int. Ed.* **2009**, *48*, 6608; *Angew. Chem.* **2009**, *121*, 6732.
- [2] *Energy for the 21st Century: A Comprehensive Guide to Conventional and Alternative Sources* (Ed.: R. L. Nersesian), M. E. Sharpe, Inc., 80 Business Park Drive, Armonk, New York, **2007**.
- [3] a) *Hydrogen as a Future Energy Carrier* (Eds.: A. Züttel, A. Borgschulte, L. Schlapbach), Wiley-VCH, Weinheim, **2008**; b) S. Enthaler, *ChemSusChem* **2008**, *1*, 801; c) F. Joó, *ChemSusChem* **2008**, *1*, 805; d) H. L. Jiang, S. K. Singh, J. M. Yan, X. B. Zhang, Q. Xu, *ChemSusChem* **2010**, *3*, 541.
- [4] a) L. Schlapbach, A. Züttel, *Nature* **2001**, *414*, 353; b) *Handbook of Hydrogen Storage* (Ed.: M. Hirscher), Wiley-VCH, Weinheim, **2010**.
- [5] a) W. Leitner, *Angew. Chem. Int. Ed. Engl.* **1995**, *34*, 2207; *Angew. Chem.* **1995**, *107*, 2391; b) T. Sakakura, J.-C. Choi, H. Yasuda, *Chem. Rev.* **2007**, *107*, 2365; c) D. J. Darensbourg, *Chem. Rev.* **2007**, *107*, 2388; d) S. Enthaler, J. Langermann, T. Schmidt, *Energy Environ. Sci.* **2010**, *3*, 1207; e) *Carbon Dioxide as Chemical Feedstock* (Ed.: M. Aresta), Wiley-VCH, Weinheim, **2010**.
- [6] a) W. Lubitz, B. Tumas, *Chem. Rev.* **2007**, *107*, 3900; b) G. J. Kubas, *Chem. Rev.* **2007**, *107*, 4152.
- [7] a) J. F. Hull, Y. Himeda, W. H. Wang, B. Hashiguchi, R. Periana, D. J. Szalda, J. T. Muckerman, E. Fujita, *Nat. Chem.* **2012**, *4*, 383; b) K. Schuchmann, V. Müller, *Science* **2013**, *342*, 1382; c) G. A. Filonenko, R. Putten, E. N. Schulp, E. J. M. Hensen, E. A. Pidko, *ChemCatChem* **2014**, *6*, 1526.
- [8] a) A. Boddien, C. Federsel, P. Sponholz, D. Mellmann, R. Jackstell, H. Junge, G. Laurenczy, M. Beller, *Energy Environ. Sci.* **2012**, *5*, 8907; b) S. F. Hsu, S. Rommel, P. Eversfield, K. Müller, E. Klemm, W. R. Thiel, B. Plietker, *Angew. Chem. Int. Ed.* **2014**, *53*, 7074; *Angew. Chem.* **2014**, *126*, 7194.
- [9] a) A. Boddien, F. Gärtner, C. Federsel, P. Sponholz, D. Mellmann, R. Jackstell, H. Junge, M. Beller, *Angew. Chem. Int. Ed.* **2011**, *50*, 6411; *Angew. Chem.* **2011**, *123*, 6535; b) G. Papp, J. Csorba, G. Laurenczy, F. Joó, *Angew. Chem. Int. Ed.* **2011**, *50*, 10433; *Angew. Chem.* **2011**, *123*, 10617.
- [10] Of particular note is the hydrogen content of 2.35 wt % for HCOONa/H<sub>2</sub>O and 2.02 wt % for HCOOK/H<sub>2</sub>O, but they are nontoxic, noncorrosive, nonflammable, and easy to handle. The volumetric hydrogen density of saturated HCOOK solution at 25°C is 28 g L<sup>-1</sup>, which is by a factor of 3.8 superior to commercial Li-ion batteries as discussed in Ref. [8a].
- [11] a) L. He, J. Ni, L. C. Wang, F. J. Yu, Y. Cao, H. Y. He, K. N. Fan, *Chem. Eur. J.* **2009**, *15*, 11833; b) Q. Y. Bi, X. L. Du, Y. M. Liu, Y. Cao, H. Y. He, K. N. Fan, *J. Am. Chem. Soc.* **2012**, *134*, 8926.
- [12] a) H. Wiener, Y. Sasson, J. Blum, *J. Mol. Catal.* **1986**, *35*, 277; b) B. Zaidman, H. Wiener, Y. Sasson, *Int. J. Hydrogen Energy* **1986**, *11*, 341.
- [13] It should be noted that along with the creation of highly strained Pd NPs in the Pd/r-GO catalysts, substantial microstructural changes of the corresponding r-GO support also occurred as a result of the palladium deposition as shown in Figures S8 and S9.
- [14] a) P. M. Ajayan, B. I. Yakobson, *Nature* **2006**, *441*, 818; b) G. M. Scheuermann, L. Rumi, P. Steuerer, W. Bannwarth, R. Mülhaupt, *J. Am. Chem. Soc.* **2009**, *131*, 8262.
- [15] C. Pham-Huu, R. Vieira, B. Louis, A. Carvalho, J. Amadou, T. Dintzer, M. J. Ledoux, *J. Catal.* **2006**, *240*, 194.
- [16] a) D. N. Belton, Y. M. Sun, J. M. White, *J. Am. Chem. Soc.* **1984**, *106*, 3059; b) K. Tedsree, T. Li, S. Jones, C. W. A. Chan, K. M. K. Yu, P. A. J. Bagot, E. A. Marquis, G. D. W. Smith, S. C. E. Tsang, *Nat. Nanotechnol.* **2011**, *6*, 302.
- [17] a) I. Kasatkin, P. Kurr, B. Kniep, A. Trunschke, R. Schlögl, *Angew. Chem. Int. Ed.* **2007**, *46*, 7324; *Angew. Chem.* **2007**, *119*, 7465; b) B. T. Sneed, C. N. Brodsky, C. H. Kuo, L. K. Lamontagne, Y. Jiang, Y. Wang, F. Tao, W. Huang, C. K. Tsung, *J. Am. Chem. Soc.* **2013**, *135*, 14691.
- [18] A. Pătru, P. Antitomaso, R. Sellin, N. Jerez, P. L. Taberna, F. Favier, *Int. J. Hydrogen Energy* **2013**, *38*, 11695.
- [19] Note that under conditions, in which the HCOOK concentration (> 8 M) or reaction temperature (> 150°C) is high, a very small amount of CO<sub>2</sub> (< 0.05 vol %) along with H<sub>2</sub> would be generated as a result of the slow transformation of bicarbonate ions to carbonate (2HCO<sub>3</sub><sup>-</sup> → CO<sub>3</sub><sup>2-</sup> + CO<sub>2</sub> + H<sub>2</sub>O).
- [20] D. B. Levin, L. Pitt, M. Love, *Int. J. Hydrogen Energy* **2004**, *29*, 173.

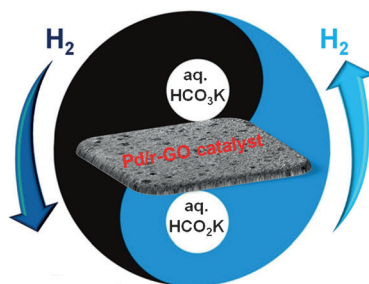
## Communications



### Hydrogen Storage

Q. Y. Bi, J. D. Lin, Y. M. Liu, X. L. Du,  
J. Q. Wang, H. Y. He,  
Y. Cao\*    

An Aqueous Rechargeable Formate-  
Based Hydrogen Battery Driven by  
Heterogeneous Pd Catalysis



**The formate/bicarbonate pair:** A rechargeable hydrogen battery based on repetitive formate/bicarbonate interconversion in aqueous solution was developed. A hybrid material of Pd nanoparticles and reduced graphite oxide serves as the robust and efficient catalyst for both steps. Multiple charging and discharging cycles were performed with comparable storage/release efficiency and the resulting  $H_2$  gas is free of CO and  $CO_2$ .